MOLECULAR AND CELLULAR BIOLOGY, Jan. 2010, p. 423–435 Vol. 30, No. 2
0270-7306/10/$12.00 doi:10.1128/MCB.01240-09

Alternative Mechanisms for Coordinating Polymerase α and MCM Helicase▽

Chanmi Lee,[1] Ivan Liachko,[1] Roxane Bouten,[2] Zvi Kelman,[2] and Bik K. Tye[1]*

Department of Molecular Biology & Genetics, Cornell University, Ithaca, New York 14853,[1] and Center for Advanced Research in Biotechnology, University of Maryland Biotechnology Institute, Rockville, Maryland 20850[2]

Received 14 September 2009/Returned for modification 9 October 2009/Accepted 2 November 2009

Functional coordination between DNA replication helicases and DNA polymerases at replication forks, achieved through physical linkages, has been demonstrated in prokaryotes but not in eukaryotes. In *Saccharomyces cerevisiae*, we showed that mutations that compromise the activity of the MCM helicase enhance the physical stability of DNA polymerase α in the absence of their presumed linker, Mcm10. Mcm10 is an essential DNA replication protein implicated in the stable assembly of the replisome by virtue of its interaction with the MCM2-7 helicase and Polα. Dominant *mcm2* suppressors of *mcm10* mutants restore viability by restoring the stability of Polα without restoring the stability of Mcm10, in a Mec1-dependent manner. In this process, the single-stranded DNA accumulation observed in the *mcm10* mutant is suppressed. The activities of key checkpoint regulators known to be important for replication fork stabilization contribute to the efficiency of suppression. These results suggest that Mcm10 plays two important roles as a linker of the MCM helicase and Polα at the elongating replication fork—first, to coordinate the activities of these two molecular motors, and second, to ensure their physical stability and the integrity of the replication fork.

The key players of the replication machinery are the DNA polymerases that synthesize the leading and lagging daughter strands and the replicative helicase that unwinds the parental strands ahead of the polymerases. Coordination between the helicase and the polymerases is critical during replication. Uncoupling of these two molecular machines, especially during lagging strand synthesis, may result in an unrestrained helicase and the exposure of extensive single-stranded DNA (ssDNA), as observed in checkpoint mutants treated with hydroxyurea (HU) (37). Although there is no direct evidence, the implication is that the replicative helicase would be moving at a faster pace than would the DNA polymerase if synchrony were destroyed. In *Escherichia coli*, the replicative helicase (DnaB) and the primase (DnaG) are coupled by direct contact to form a tight complex (3). In T7, processivity of the gp5 polymerase in lagging strand synthesis requires coupling to the gp4 helicase (16). Recent studies of the budding yeast *Saccharomyces cerevisiae* suggest that Mrc1 may couple DNA polymerase ε and the MCM helicase on the leading strand as well as activate the checkpoint response under replication stress (1, 22, 28). A candidate for coupling DNA polymerase α primase and the MCM helicase on the lagging strand is Mcm10, because Mcm10 interacts with subunits of the Mcm2-7 helicase (26, 29) as well as Polα (14, 33) and the stability of Polα requires Mcm10 in both budding yeast and human cells (8, 33). Mcm10 is an essential protein known to be involved in various aspects of the replication process. It is required during both initiation and elongation steps of DNA replication and interacts with a wide range of replication factors, such as ORC (17, 23, 29), MCM helicase, DNA polymerases ε and δ (23), Cdc45 (34), and Polα (33). Therefore, Mcm10 is important for the overall stability of the elongation complex, but its essential function remains unknown.

Accumulating evidence suggests that the major function of many checkpoint proteins is the stabilization of the replication machinery at the fork (9, 22, 39), in addition to regulation of the temporal and spatial firing of origins and prevention of premature mitosis (31, 35, 39). The main signal that leads to checkpoint activation is believed to be the exposure of RPA-coated ssDNA (42). In *Xenopus*, ssDNA exposure has been shown to be mediated by a functional uncoupling between the polymerase and the helicase (7), and it has been shown that the level of checkpoint activation depended on the extent of ssDNA accumulation. This observation suggests that uncoupling of the polymerase and the helicase activity would result in ssDNA accumulation that in turn would activate the checkpoint pathway to stabilize the fork.

In our study, we carried out a random and a gene-targeted mutagenesis screen to identify mutations that suppress the conditional lethality of *mcm10* caused by the lability of Mcm10 in budding yeast (27). We found suppressor mutations in *MCM2*, which encodes one of the six distinct subunits of the MCM helicase. These *mcm2* mutations correct the fork defects of *mcm10*, particularly that which leads to Polα instability. The altered helicase activity and activation of the checkpoint pathway of the *mcm2* mutants appeared to be required for viability of *mcm10 mcm2*. We showed that uncoupling the MCM helicase and DNA polymerase α by destabilizing Mcm10 leads to accumulation of ssDNA, which is suppressed by reducing the MCM helicase activity. Our findings suggest that the physical coupling of Polα and the helicase by Mcm10 may be replaced by an alternative stabilization mechanism that involves slowing down the helicase and activating the checkpoint proteins.

* Corresponding author. Mailing address: 321 Biotechnology Bldg., Ithaca, NY 14853. Phone: (607) 255-2445. Fax: (607) 255-6249. E-mail: bt16@cornell.edu.

▽ Published ahead of print on 16 November 2009.

TABLE 1. Strains used in this study

Strain isogenic to W303	Description	Source
W303-1A	*MAT***a** *ade2-1 trp1-1 can1-100 leu2-3,112 his3-11,15 ura3-1*	R. Rothstein
W303-1B	*MATα ade2-1 trp1-1 can1-100 leu2-3,112 his3-11,15 ura3-1*	R. Rothstein
BTY100	W303 *MAT***a** *mcm10-1*	This lab
BTY101	W303 *MATα mcm10-1*	This lab
BTY103	W303 *MAT***a** *mcm10-43*	This lab
BTY102	W303 *MATα mcm10-43*	This lab
ILY230	*MAT***a** *13myc-MCM10 TRP1*	This lab
ILY232	*MAT***a** *13myc-mcm10-43 TRP1*	This lab
SSY84	*MAT***a** *13myc-mcm10-1 HIS3MX*	This lab
CLY88	*MAT***a** *13myc-mcm10-43 TRP1 mcm2-G400D*	This study
CLY90	*MAT***a** *13myc-mcm10-1 HIS3MX mcm2-G400D*	This study
CLY91	W303 *MAT***a** *mcm2-P399L*	This lab
CLY92	W303 *MAT***a** *mcm2-G400D*	This lab
CLY93	W303 *MATα mcm2-D472G*	This lab
CLY94	W303 *MAT***a** *mcm2-R617H*	This lab
ILY215	W303 *MAT***a** *mcm2-S619F*	This lab
CLY95	W303 *MAT***a** *mcm2-P399L mcm10-1*	This study
CLY96	W303 *MATα mcm2-G400D mcm10-1*	This study
CLY97	W303 *MATα mcm2-D472G mcm10-1*	This study
CLY98	W303 *MATα mcm2-R617H mcm10-1*	This study
ILY245	W303 *MAT***a** *mcm2-S619F mcm10-1*	This study
XL16	W303 *MAT***a** *rad53::URA3 sml1::HIS3*	This lab
XL18	W303 *MAT***a** *mec1::LEU2 sml1::URA3*	This lab
XL232	W303 *MATα sgs1::URA3*	This lab
XL158	W303 *MATα srs2::HIS3*	This lab
CLY99	W303 *MAT***a** *exo1::URA3*	This study
CLY84	W303 *MAT***a** *mre11::LEU2*	This lab
CLY102	W303 *MAT***a** *mcm10-1 rad53::URA3 sml1::HIS3*	This study
CLY103	W303 *MAT***a** *mcm10-1 mec1::LEU2 sml1::URA3*	This study
CLY105	W303 *MATα mcm10-1 sgs1::URA3*	This study
CLY108	W303 *MATα mcm10-1 exo1::URA3*	This study
CLY85	W303 *MAT***a** *mcm10-1 mre11::LEU2*	This study
CLY113	W303 *MAT***a** *mcm2-G400D rad53::URA3 sml1::HIS3*	This study
CLY114	W303 *MATα mcm2-G400D mec1::LEU2 sml1::URA3*	This study
CLY116	W303 *MAT***a** *mcm2-G400D sgs1::URA3*	This study
CLY119	W303 *MAT***a** *mcm2-G400D exo1::URA3*	This study
CLY120	W303 *MAT***a** *mcm2-G400D srs2::HIS3*	This study
CLY86	W303 *MAT***a** *mcm2-G400D mre11::LEU2*	This study
CLY125	W303 *MAT***a** *mcm2-G400D mcm10-1 rad53::URA3 sml1::HIS3*	This study
CLY126	W303 *MATα mcm2-G400D mcm10-1 mec1::LEU2 sml1::URA3*	This study
CLY128	W303 *MATα mcm2-G400D mcm10-1 sgs1::URA3*	This study
CLY131	W303 *MAT***a** *mcm2-G400D mcm10-1 exo1::URA3*	This study
CLY132	W303 *MAT***a** *mcm2-G400D mcm10-1 srs2::HIS3*	This study
CLY87	W303 *MAT***a** *mcm2-G400D mcm10-1 mre11::LEU2*	This study
CLY152	W303 *MAT***a** *3×HA-Cdc17 HIS3*	This study
CLY144	W303 *MATα 3×HA-Cdc17 HIS3 mcm10-1*	This study
CLY145	W303 *MATα 3×HA-Cdc17 HIS3 mcm10-1 mcm2-G400D*	This study
CLY148	W303 *MAT***a** *3×HA-Cdc17 HIS3 mec1*	This study
CLY149	W303 *MAT***a** *3×HA-Cdc17 HIS3 mec1 mcm10-1 mcm2-G400D*	This study
CLY140	W303 *MAT***a** *3×HA-Rad53 kanMX*	This study
CLY141	W303 *MATα 3×HA-Rad53 kanMX mcm10-1*	This study
CLY142	W303 *MAT***a** *3×HA-Rad53 kanMX mcm2-G400D*	This study
CLY143	W303 *MATα 3×HA-Rad53 kanMX mcm10-1 mcm2-G400D*	This study
CLY150	W303 *MAT***a** *3×HA-Cdc17 HIS3 rad53*	This study
CLY151	W303 *MAT***a** *3×HA-Cdc17 HIS3 rad53 mcm10-1 mcm2-G400D*	This study
CLY152	W303 *MAT***a** *ADE2 RFA1-8ala-YFP*	R. Rothstein
CLY153	W303 *MATα ADE2 RFA1-8ala-YFP mcm10-1*	This study
CLY154	W303 *MAT***a** *ADE2 RFA1-8ala-YFP mcm2-G400D*	This study
CLY155	W303 *MATα ADE2 RFA1-8ala-YFP mcm10-1 mcm2-G400D*	This study

MATERIALS AND METHODS

Strains and plasmids. Strains used in this study are listed in Table 1. All strains were isogenic derivatives of W303-1A, unless otherwise indicated. Strains carrying various deletions were made by crossing the *mcm10-1 mcm2* strain with the appropriate deletion strain and selecting desired segregants by their conditional phenotypes and/or auxotrophy and by sequencing. Genotypes were confirmed by PCR, sequencing, or by plasmid complementation, where applicable. Plasmids used in this study are listed in Table 2. Plasmids used for yeast two-hybrid analysis were constructed by the Gateway system (Invitrogen, San Diego, CA). The Gateway recombination cassette was inserted into the BamHI site of pGAD2F and pBTM116 plasmids (13) for conversion into destination vectors.

Suppressor screen. Suppressor screenings for random suppressor mutations of *mcm10-1* were carried out as described previously (27). Plasmid-based mutagenesis of *MCM2* was subsequently carried out to screen for more suppressor

TABLE 2. Plasmids used in this study

Plasmid	Description	Source
pRS315	YCP LEU2	New England Biolabs
pRS315MCM10	YCP LEU2 MCM10	This lab
pRS315mcm2-G400D	YCP LEU2 *mcm2-G400D*	This lab
pRS316MCM10	YCP URA3 MCM10	This lab
pGAD2F	2μm LEU2 GAD4-AD	S. Fields
pBTM116	2μm TRP1 LEXA-DBD	S. Fields
pSH18-34	URA3 LacZ with LEXA binding sites	S. Fields
pGADgw	pGAD2F with Gateway cassette	This lab
pBTMgw	pBTM116 with Gateway cassette	This lab
pGBKgw	pGBKT7 with Gateway cassette; Amp^r	This lab
pBTMMCM10	pBTMgw *MCM10*	This lab
pBTMmcm10-1	pBTMgw *mcm10-1*	This lab
pBTMMCM2	pBTMgw *MCM2*	This lab
pBTMmcm2-G400D	pBTMgw *mcm2-G400D*	This lab
pBTMmcm2-S619F	pBTMgw *mcm2-S619F*	This lab
pGADMCM10	pGADgw *MCM10*	This lab
pGADmcm10-1	pGADgw *mcm10-1*	This lab
pGADMCM2	pGADgw *MCM2*	This lab
pGADmcm2-G400D	pGADgw *mcm2-G400D*	This lab
pGADmcm2-S619F	pGADgw *mcm2-S619F*	This lab
YCp1	*LEU2 CENV ARS1*	This lab

mutations. *MCM2* was cloned into the pRS316 plasmid and mutagenized in *Escherichia coli* by using XL1-red competent cells (Stratagene). Mutagenized plasmids were obtained from *E. coli*, transformed into *mcm10-1*, and plated at 37°C to select for suppressors. The plasmids were sequenced to determine the nature of the mutations.

Expression and purification of MCM mutant proteins. All *Methanothermobacter thermautotrophicus* MCM mutant proteins used in this study are derivatives of the full-length enzyme and were generated using the QuikChange site-directed mutagenesis kit (Stratagene), using the full-length MCM in the pET-21a vector (Novagen). All constructs contain a C-terminal His_6 tag. The oligonucleotides used for the mutagenesis are G190D forward, 5′-AACCTTTC CGGTGATGAACAGCCCCGG-3′; G190D reverse, 3′-CCGGGGCTGTTCA TCACCGGAAAGGTT-5′; R392H forward, 5′-CGTGAGGAGGACCACTCA GCCATACAC-3′; and R392H reverse, 3′-GTGTATGGCTGAGTGGTCCTC CTCACG-5′. The wild-type and mutant proteins were overexpressed in codon plus cells (Stratagene) at 16°C and purified as previously described (21).

DNA helicase assay. Substrates for the helicase assay were generated as previously described (36) by hybridizing two oligonucleotides (DF50, 5′-GGGACG CGTCGGCCTGGCACGTCGGCCGCTGCGGCCAGGCACCCGATGGC-3′, and DF25F, 5′-CCGACGTGCCAGGCCGACGCGTCCC-3′). DF25F was labeled using [γ-^{32}P]ATP (PerkinElmer) and T4 polynucleotide kinase (Fermentas) and hybridized to DF50, and the substrate was purified as previously described (36). Helicase assays were performed as previously described in reaction mixtures (15 μl) containing 20 mM Tris-HCl (pH 8.0), 10 mM $MgCl_2$, 2 mM dithiothreitol (DTT), 100 μg/ml bovine serum albumin (BSA), 3.33 mM ATP, 10 fmol of ^{32}P-labeled DNA substrate, and MCM proteins, as indicated in the figure legends. Mixtures were incubated at 60°C for 30 min. Reactions were stopped by adding 5 μl of buffer containing 1% sodium dodecyl sulfate (SDS), 100 mM EDTA, 0.1% xylene cyanol, 0.1% bromophenol blue, and 50% glycerol, and then placed on ice. Aliquots were fractionated on an 8% native polyacrylamide gel in 0.5× TBE (45 mM Tris, 45 mM boric acid, 1 mM EDTA) and electrophoresed for 1 h at 150 V at 25°C. The helicase activity was visualized and quantitated by phosphorimaging.

Protein-protein interactions. The wild-type W303 strain with the pSH18-34 reporter plasmid was transformed with pGAD2F and pBTM116 constructs for the two-hybrid assay (13). Transformants were selected on the appropriate dropout plates. Interactions were assessed by the appearance of blue colonies on plates containing X-Gal (5-bromo-4-chloro-3-indolyl-β-D-galactopyranoside; Sigma). Relevant strains were inoculated for saturated cultures and spotted onto X-Gal plates and photographed after 2 to 4 days of growth at 30°C.

Plasmid stability assays. MCM assays were carried out as described in reference 12. Wild-type and mutant strains were transformed with the plasmid YCp1 that contains an origin of replication (*ARS1*), a centromere, and the *LEU2* selectable marker. Assessment of plasmid loss rate in the mutants was done as described.

2D DNA gel electrophoresis. Protocols for two-dimensional (2D) DNA gel electrophoresis were adapted from the method of Huberman (18) and the rapid DNA purification method (40). Cells were broken and spheroplasts were collected by centrifugation for 10 min at 8,000 rpm (4°C) according to the neutral-neutral method. The spheroplasts were resuspended in G_2 buffer (Qiagen), and subsequent steps were carried out according to the rapid DNA purification method.

For visualization of replication intermediates at the *ARS1* region, purified DNA was digested to completion with NcoI to produce a 5-kb fragment. To enrich the sample for replicating DNA, digested DNA was passed through BND cellulose (Sigma-Aldrich) columns as described in reference 11. *ARS1* probes were made by amplifying a 1.5-kb region centered at *ARS1* by PCR. The probes were radiolabeled with [α-^{32}P]dATP by using the Prime-It II random primer labeling kit from Stratagene.

Western blot analysis. Cdc17 was tagged with 3×HA at the C terminus. Mcm10 in wild-type, *mcm10-1*, and *mcm10-43* strains was tagged with 13×myc and introduced into *mcm2-G400D* or *mcm2-S619F* strains. The strains were grown to log phase at 30°C and subsequently shifted to 37°C. Samples were collected at various time points for Western blot analysis. Proteins were extracted either by treating the cells briefly with mild alkali and then boiling in SDS-polyacrylamide gel electrophoresis (PAGE) sample buffer as described in reference 25 or by glass bead lysis in the presence of protease inhibitors. Extraction of phosphorylated Rad53 also contained phosphatase inhibitors. The mild-alkali-treatment (0.2 M NaOH) method produced a protein extraction yield similar to that of glass bead lysis. Mouse anti-myc (Santa Cruz) and mouse anti-hemagglutinin (HA; Roche) antibodies were used to probe for the appropriate myc-tagged and HA-tagged proteins. Goat anti-mouse horseradish peroxidase-conjugated secondary antibodies were obtained from Bio-Rad. Blots were visualized by chemiluminescence reagents (Promega).

FACS. For overall ratio of cells in G_1, S, or G_2 phase, log-phase cells of wild-type, *mcm10-1*, *mcm2-G400D*, and *mcm10 mcm2* strains were collected without α-factor arrest. For cell cycle progression, log-phase cultures were arrested in G_1 phase by α-factor for 2 h. Cells were spun down and resuspended in fresh yeast extract-peptone-dextrose (YPD) media containing 100 μg/ml of pronase (Sigma) for rapid α-factor degradation and release into S phase. The G_1-arrested cells were released at either 30°C or 37°C. For the latter, the cells were preincubated at 37°C for 1 h before release to allow Mcm10 degradation to occur before the onset of S phase. Samples at different time points were collected for fluorescence-activated cell sorting (FACS) analysis at the Cornell FACS facility.

Fluorescence microscopy. Visualization of yellow fluorescent protein (YFP)-conjugated RPA was carried out in live cells under a conventional fluorescence microscope with a 100× objective. The images were obtained with a charge-coupled-device (CCD) detector by using Openlab (Improvision). Log-phase cells

were prepared by growing in synthetic media at 30°C or subsequent exposure at 37°C for 2 h.

RESULTS

Mutations in *MCM2* that suppress *mcm10* TS affect the helicase activity. Two temperature-sensitive (TS) mutants with *MCM10*, *mcm10-1*(*P269L*), and *mcm10-43*(*C320Y*) mutations share many of the same phenotypes (17). Both mutants show reduced replication initiation activity and fork pausing at unfired replication origins at the permissive temperature but arrest in S phase at the restrictive temperature. The protein products of both mutant alleles are heat labile (33, 34), suggesting that the instability may be the cause of these phenotypes. To determine the essential role of Mcm10 that was compromised at the restrictive temperature, two suppressor screens for *mcm10* TS were carried out (27). In the first screen, spontaneous TS suppressors that have simultaneously acquired cold sensitivity (CS) were isolated. They all lie in *MCM2* at two positions, R617 and S619, and they are all dominant suppressors (27). To identify other mutations in *MCM2* that suppress the TS phenotype of *mcm10*, but did not necessarily have a CS phenotype, a CEN plasmid carrying *MCM2* was randomly mutagenized and transformed into *mcm10* cells. The transformation reaction mixture was plated at 37°C for identification of dominant suppressors. The resultant suppressor alleles were sequenced and integrated into the genomes of both wild-type and *mcm10* cells. In all, 10 dominant suppressors comprising six alleles were isolated. Nine out of the 10 mutations clustered in two regions of *MCM2* at either the region from P399 to R401 or that from R617 to S619 (Fig. 1A, panel i). With the exception of the P399L mutant, these *mcm2* mutants do not display TS on their own (Fig. 1A, panel ii). Spot dilution of the mutants shows that the outlier D472G mutation is least able to suppress *mcm10-1* TS. The *mcm2* mutants are all allele-nonspecific suppressors, as they suppress both *mcm10-1* and *mcm10-43* (Fig. 1A, panel i). As both *mcm10-1* and *mcm10-43* express unstable forms of the protein that degrades at the restrictive temperature, we speculated that suppression by the *mcm2* mutants may involve either restoration of Mcm10 stability or compensatory changes which lead to increased affinity between the proteins or bypass of function.

Most of the *mcm2* suppressor mutations are located in regions of Mcm2 that are conserved throughout archaeal and eukaryotic MCM helicase (Fig. 1A, panel iii). In particular, the residues G400 and R617 in eukaryotic *MCM2* are highly conserved in all eukaryotic MCM2-7 subunits and the archaeal MCM protein. Based on a recent study of the archaeal MCM helicase crystal structure from *Sulfolobus solfataricus* (5), these two regions are at the interface of adjacent subunits of the MCM helicase with the residue corresponding to *S. cerevisiae* G400 (ScG400) of one subunit juxtaposed to the residue corresponding to ScR617 of the neighboring subunit (Fig. 1B). The positions of the mutated residues suggest that suppression of *mcm10* TS by the different *mcm2* mutations may occur through a common mechanism and may involve altered interaction between the subunits at that particular interface.

The corresponding ScG400D and ScR617H mutations were individually introduced into the archaeal MCM protein for *in vitro* helicase assays to determine how they would affect the helicase activity. The helicase activity was measured by the extent of strand displacement when the substrate double-stranded DNA (dsDNA) was incubated with the purified proteins. The mutant helicases displayed weaker helicase activity than did the wild type (Fig. 2A and B). Keeping in mind that the archaeal MCM helicase is a homohexamer, the effect of an *mcm2* equivalent mutation in the archaeal MCM is likely amplified. Therefore, the helicase defect of these two *mcm2* suppressors in yeast is likely to be subtle, as the suppressors showed no obvious growth defects (Fig. 1A, panel i).

The archaeal MCM helicase result supports the *in vivo* minichromosome maintenance (*mcm*) assay result of the budding yeast MCM helicase. The *mcm* assay is used to assess the general replication proficiency of yeast cells and measures how well the cells are able to replicate and maintain plasmids in the absence of selective pressure. Mutants defective in replication display higher levels of plasmid loss. The *mcm2* mutants displayed various degrees of *mcm* defect, independent of *mcm10-1* (Fig. 2C). The result shows that the corresponding mutations that decreased helicase activity in the archaeal MCM helicase also showed a modest reduction in replication proficiency in the budding yeast. These observations suggest that although the decreased helicase activity compromises the replication efficiency of the *mcm10* mutant at the permissive temperature, it is important for rescuing the lethal effects of *mcm10* at the nonpermissive temperature.

***mcm2* suppressors do not restore Mcm10-1 protein-protein interactions or stability.** Mcm10 interacts with the Mcm2-7 subunits (17, 29), but this interaction is disrupted in the *mcm10-1* strain. To investigate whether the *mcm2* suppressors restore this interaction, we performed a yeast two-hybrid analysis of the Mcm2 suppressors, *mcm2-G400D* and *mcm2-S619F*, with the Mcm10-1 protein (Fig. 3A). We found that the level of interaction between the mutant Mcm2 construct and wild-type Mcm10 construct was similar to that of wild-type Mcm2 and wild-type Mcm10 interaction. However, we could not detect interaction between the *mcm10-1* and *mcm2* constructs. This result suggests that the protein interaction between Mcm10 and Mcm2 is not restored by the *mcm2* mutations.

Although the *mcm2* suppressor mutations did not restore physical interactions with Mcm10-1, we wanted to know if they restored the stability of the mutant Mcm10 protein at 37°C, a suspected cause of the TS phenotype of *mcm10* cells. Mcm10 protein levels in the wild-type, *mcm10*, and *mcm10 mcm2* suppressor strains were visualized by Western blots. Both Mcm10-1 and Mcm10-43 proteins were labile in the presence or absence of the *mcm2* suppressor mutations (Fig. 3B). Therefore, the *mcm2* suppressors do not prevent the degradation of either Mcm10-1 or Mcm10-43 proteins.

Since the *mcm2* suppressors did not restore their interactions with the mutant Mcm10 protein or prevent its degradation, we asked if Mcm10 is dispensable in the *mcm2* suppressor strains. We used an *mcm10* knockout strain that was kept viable by a wild-type copy of *MCM10* on a plasmid and determined whether we could replace the plasmid carrying *MCM10 URA3* with one carrying *mcm2-G400D LEU2* by plasmid shuffling (Fig. 3C). We found that *mcm10* knockout strains required the *MCM10* plasmid regardless of the presence or absence of *mcm2-G400D*, suggesting that the *mcm2* suppressor could not bypass all of the essential functions of *MCM10* but

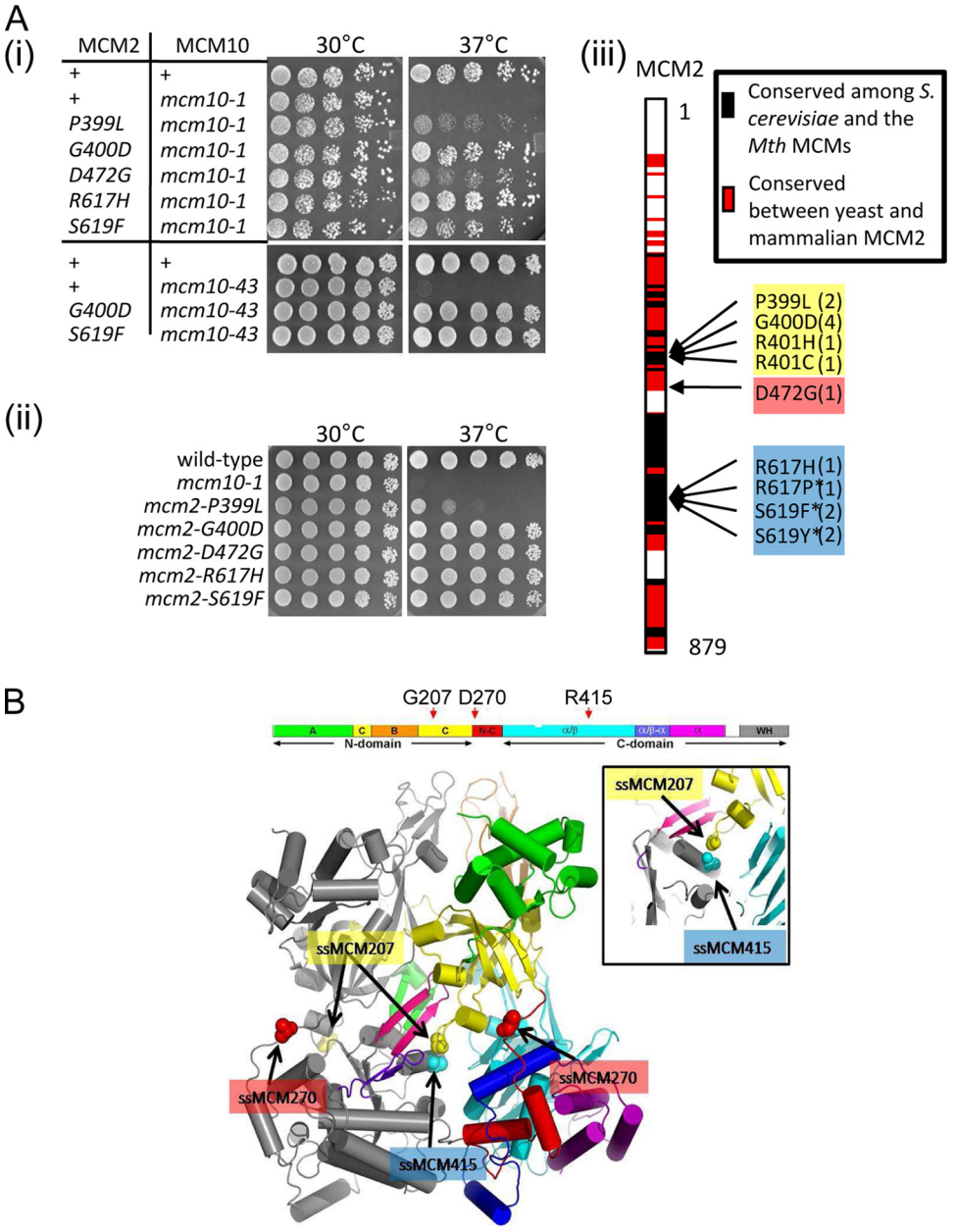

FIG. 1. Suppression of *mcm10* TS by *mcm2* mutants. (A) (i) Fivefold serial dilutions of wild-type, *mcm10-1*, and *mcm10-43* cells and the different *mcm2* suppressors in the *mcm10-1* or *mcm10-43* background were spotted onto YPD plates and incubated for 1 to 2 days at either 30°C or 37°C. The *mcm2* mutants are non-allele-specific suppressors of both *mcm10-1* and *mcm10-43*. (ii) *mcm2* suppressors, except *mcm2-P399L*, do not display TS. (iii) *mcm2* mutants are located in two specific regions of the gene. Numbers in parentheses indicate the number of times a specific mutation was independently isolated. The mutations and their corresponding positions in the three-dimensional (3D) structure shown in panel B are color coded in shades of yellow, red and blue. Asterisks mark the mutants that display cold sensitivity. (B) The corresponding residues for the well-conserved ScG400, ScD472, and ScR617 in the archaeal *Sulfolobus solfataricus* are G207, D270, and R415, respectively. The red arrows indicate the locations of the three residues within the primary structure. The residues are located in the SsMCM structure by Brewster et al. (5). G207 and R415 of adjacent subunits are localized close in space at the subunit interface.

only the essential function of *mcm10-1* and *mcm10-43* compromised at the restrictive temperature of 37°C.

***mcm2* suppressors suppress multiple replication fork defects of *mcm10*.** Replication forks in *mcm10-1* pause at unfired origins as shown by the accumulation of DNA replication intermediates near the origin sequences of *ARS1* or *ARS121* in 2D gel electrophoresis analysis (2, 29). The locations of the pauses suggest that a defect in the elongation machinery may have compromised the fork's ability to move past bound prereplication complexes (pre-RCs) at unfired origins. The accumulation of the pause structures in *mcm10-1* is more striking at 30°C than at 25°C (Fig. 4A), suggesting that the severity of fork pausing at the restrictive temperature may be the cause of death.

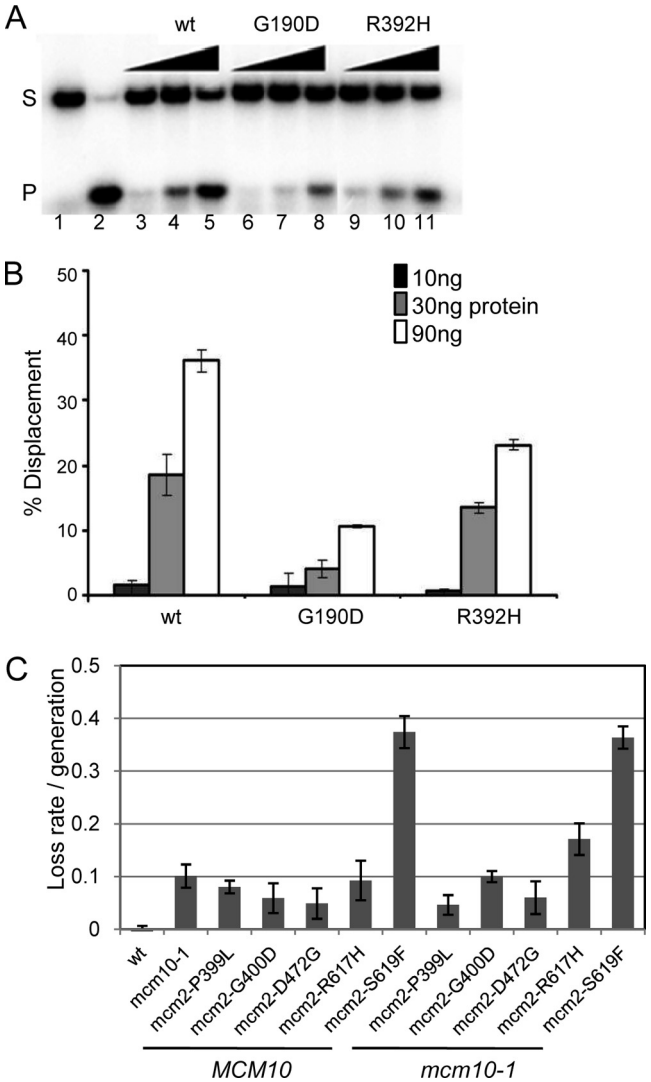

FIG. 2. Suppressor mutations affect the helicase activity. (A) Wild-type and mutant *M. thermautotrophicus* (mt) MCM proteins were purified, and helicase assays were performed. A partial duplex DNA substrate was made by hybridization of 50-mer and 25-mer ssDNAs. The extent of helicase activity was determined by measuring the displacement of the radiolabeled 25-mer from the 50-mer. Lanes 3 to 5, wild-type MCM protein; lanes 6 to 8, G190D (ScG400D) mtMCM protein; lanes 9 to 11, R392H (ScR617H) mtMCM protein; lane 1, substrate only; lane 2, boiled substrate; lanes 3, 6, and 9, 10 ng (8.7 nM as monomers) MCM protein; lanes 4, 7, and 10, 30 ng (26 nM as monomers) MCM protein; lanes 5, 8, and 11, 90 ng (78 nM as monomers) MCM protein. S, substrate; P, product. (B) Average of the results for three independent experiments. (C) *mcm* assay to measure plasmid loss rate of *mcm2* mutants at 30°C. The *mcm2* suppressors show a minichromosome maintenance defect independent of the *mcm10* mutation.

If fork pausing were indeed associated with *mcm10* TS, it would be suppressed by *mcm2*. Therefore, we asked whether the *mcm2* mutants are able to suppress the pause phenotype. Replication intermediates of wild-type, *mcm10-1*, *mcm2-G400D*, and *mcm10 mcm2* strains grown at 30°C were analyzed by 2D gel electrophoresis (Fig. 4B). The pause signals observed in *mcm10-1* strains were no longer observed in the *mcm10 mcm2* strains, suggesting that the *mcm2* suppressor has alleviated the fork pausing at unfired pre-RC. Furthermore, the enhancement rather than the suppression of the replication initiation defect (reduced bubble signal intensity) in the double mutant suggests that the lethality of *mcm10-1* at the restrictive temperature is not due to replication initiation at the origins. Failure to suppress the replication initiation defect and suppression of the pause phenotype were also observed with *mcm2-S619F* (data not shown). This result suggests that the defect of *mcm10* that leads to replication fork pausing and TS is in replication elongation.

HU depletes nucleotide pools and causes replication forks to stall. Methylmethane sulfonate (MMS) is a DNA alkylating reagent that causes DNA damage. Defects in replication fork stabilization and DNA repair have been associated with sensitivity to these chemicals (10, 38). Sensitivity to HU reflects defects in the replication fork, and sensitivity to MMS may be due to defects either in the fork or in DNA repair. We found that *mcm10-1* is sensitive to both HU and MMS and the *mcm2-G400D* suppressor alleviates this sensitivity to both reagents (Fig. 4C). The sensitivity to these reagents is more likely to be associated with the defect at the fork rather than with DNA repair because *mcm10-1* does not display increased spontaneous mutation rate by the canavanine assay (data not shown). These results further suggest that *mcm10* compromises the replication fork and that this fork defect is compensated by the *mcm2* mutation.

The observation that *mcm10* loses viability as the cells go through S phase at the restrictive temperature (2) suggests that DNA damage accumulates as the defective replication fork progresses. Therefore, the defective fork in *mcm10* may be creating damage and *mcm2* may be preventing such damage from being formed. The damage could be in the form of double-strand breaks or altered fork structures. If so, proteins that function in dsDNA break (DSB) repair or resolution of aberrant fork structures should be required in *mcm10*.

In searching for gene deletions in strains that showed synthetic growth defect or lethality with *mcm10-1*, we found *mre11*, *rad50*, *sgs1*, *exo1*, and *srs2* (Fig. 4D). Even at 30°C, strains with *mre11*, *rad50*, *sgs1*, and *exo1* deleted displayed synthetic growth defects with *mcm10-1*. Also, *mcm10 srs2* is synthetically lethal; the strain is viable only when it carries a plasmid expressing the wild-type *MCM10* gene. *MRE11* and *RAD50* are required during the initial processing of DSB repair (32). DNA helicases *SGS1*, *SRS2* and nuclease *EXO1* process ssDNA overhangs during DSB repair (19, 20). It has been previously reported that *mcm10-1* is synthetically lethal with yet another DNA helicase/nuclease *dna2-2* (2) that also functions in DSB repair.

However, Sgs1, Exo1, and Srs2 also function in fork repair as their helicase or nuclease activities are involved in promoting progression and/or resolution of reversed forks and Holliday junction structures. Srs2 is known to disrupt Rad51 binding to ssDNA to prevent aberrant recombination (24) and most *srs2* synthetic lethal mutants are rescued by deletion of *rad51* (15). Indeed, we observed that *rad51*Δ suppresses the *mcm10 srs2* synthetic lethality as well (data not shown). Interestingly, *mcm2-G400D* also rescues this synthetic lethality (Fig. 4D). If rescue of *mcm10 srs2* synthetic lethality by *rad51*Δ is due to disruption of Rad51 filament formation and prevention of ab-

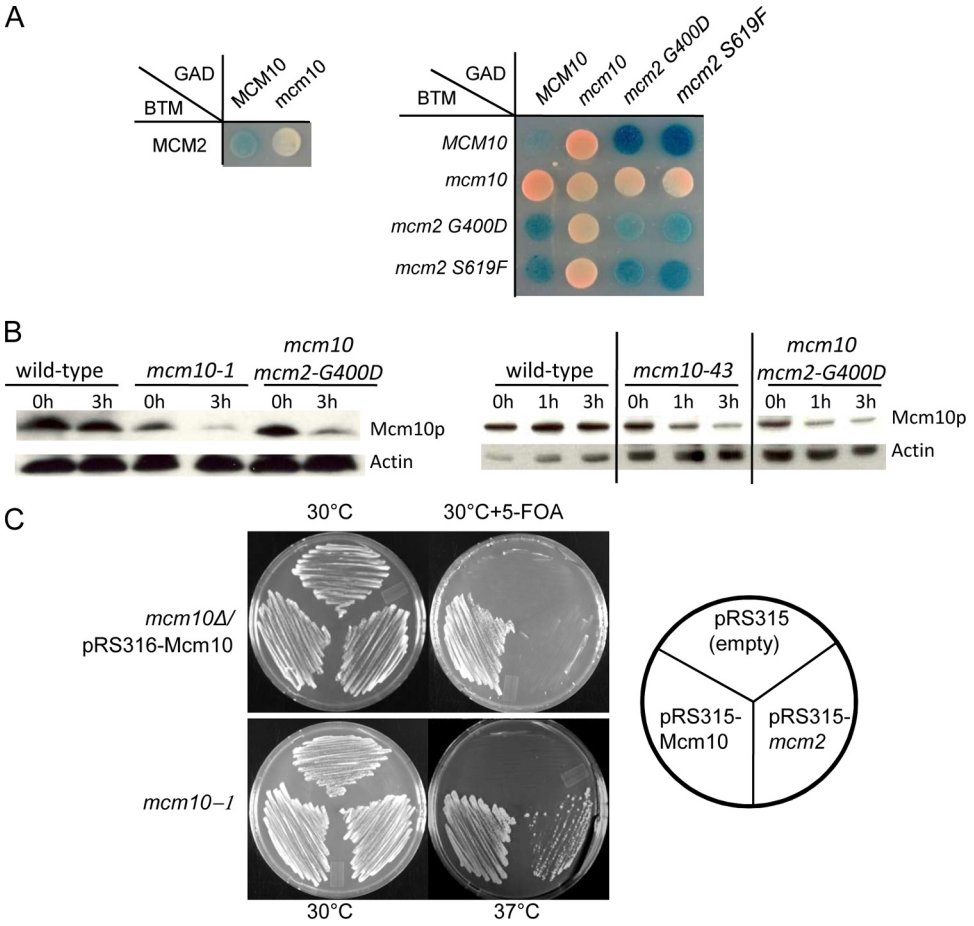

FIG. 3. Mutations in Mcm2 do not restore interaction with Mcm10-1 or stabilize the mutant Mcm10 protein. (A) Two-hybrid reporter constructs with *mcm10* and *mcm2* alleles were transformed into a wild-type W303 strain. Two-hybrid interactions are detected by blue color. The loss of interaction between Mcm10-1 and Mcm2 is not restored by Mcm2-G400D or Mcm2-S619F proteins. (B) Western blot analysis of myc-tagged Mcm10, Mcm10-1, or Mcm10-43 from wild-type and *mcm2-G400D* log-phase cells at 37°C. (C) Plasmid shuffling to determine whether the *mcm2-G400D* suppressor can substitute for the wild-type *MCM10* gene in an *mcm10* null strain. *mcm10*Δ/pRS316-*MCM10* (*URA3*) was transformed with an empty pRS315-LEU2, pRS315-Mcm10, and pRS315-mcm2-G400D and plated onto 5-fluoroorotic acid (5-FOA) plates. A control experiment shows that pRS315-mcm2-G400D is functional and is able to suppress *mcm10-1* TS.

errant recombination events, then *mcm2* may be preventing *mcm10* from producing substrates for Srs2 and/or Rad51.

We observed that *mcm2-G400D* also suppresses *mcm10 sgs1* and *mcm10 exo1* growth defects (Fig. 4D), suggesting that the DNA helicases/nucleases that are important for the viability of *mcm10* are no longer vital in *mcm2-G400D* cells. However, *mcm2-G400D* does not suppress *mcm10 mre11* or *mcm10 rad50* synthetic defect (Fig. 4D), which indicates that DSBs are still occurring in *mcm10 mcm2*. In summary, these results suggest that the role of Sgs1, Exo1, and Srs2 in *mcm10* is different from that of Mre11 and Rad50, implying that different types of damage are occurring at the replication fork due to *mcm10* defect.

Checkpoint proteins are required for the suppression of *mcm10-1*. The nature of the various *mcm10* phenotypes that are suppressed by *mcm2* strongly suggests that the defect in the replication fork is the cause of cell death at the restrictive temperature. However, the suppressors do not suppress the TS by restoring physical interaction between the mutant Mcm10 and Mcm2 proteins or by preventing degradation of the mutant Mcm10 protein (Fig. 3). Therefore, the mechanism by which mutations in *mcm2* restore viability of *mcm10* cells at the restrictive temperature must involve mechanisms that compensate for the function of Mcm10 at the fork. One possible scenario is that Mcm10 is an important fork stabilizer. Mutations in factors that can stabilize the fork independently of Mcm10 would appear as suppressors of *mcm10-1*. Another is that Mcm10 may be essential for fork repair and the suppressor has gained the function to facilitate fork repair by alternative mechanisms. These hypotheses may be tested by candidate mutations from the different DNA repair and checkpoint pathways that negate or weaken the suppression of *mcm10* TS by the *mcm2* mutants. We introduced deletions of *mec1*, *rad53*, *rad51*, *mrc1*, *tof1*, *rad6*, *dnl4*, *rad9*, *exo1*, *mre11*, *sgs1*, *srs2*, and *ddc1* into the wild-type, *mcm10-1*, *mcm2-G400D*, and *mcm10 mcm2* strains (Fig. 5A) (results not shown for double mutants with no effect). In addition to *mre11* and *rad50*, gene deletions that have negative effects on suppression were *rad53* and *mec1*. Since both *rad53* and *mec1* also require *sml1* deletion for viability, we confirmed that *sml1* is not responsible for the negative effect on suppression (data not shown).

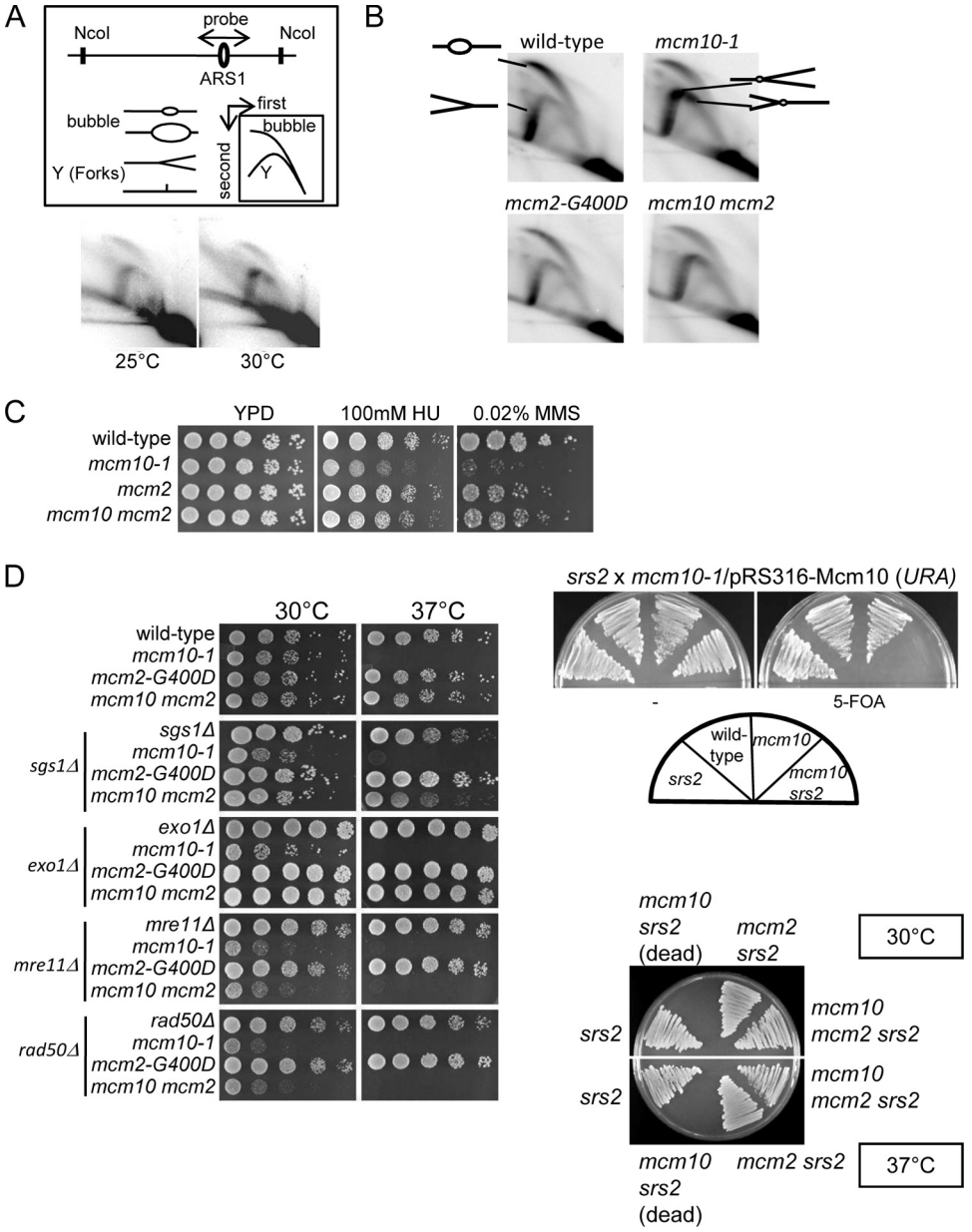

FIG. 4. Suppression of replication elongation defects of *mcm10* by *mcm2*. (A) (Top) Schematic of Southern blot of 2D gel probed with ARS1 DNA. (Bottom) DNA from log-phase cultures of *mcm10-1* cells grown at either 25°C or 30°C was analyzed by 2D gel. The arrow points to pause signal corresponding to replication intermediates accumulated in *mcm10-1* at unfired ARS1 at 30°C. This pause signal is not observed at 25°C. (B) DNAs from wild-type, *mcm10-1*, *mcm2-G400D*, and *mcm10 mcm2* cells grown at 30°C were analyzed by 2D gel. *mcm2-G400D* alleviates the pause signal, but not the initiation defect of *mcm10-1*. (C) HU and MMS sensitivity of *mcm10-1*. Fivefold serial dilutions of wild-type and mutant strains were spotted onto YPD, YPD with 100 mM HU, and YPD with 0.02% MMS. *mcm10-1* displays HU and MMS sensitivity, which is rescued by *mcm2*. (D) Cells expressing *mcm10-1* display synthetic growth defects with genes in DSB and fork repair pathway. Those expressing *sgs1*, *exo1*, *mre11*, and *rad50* display synthetic growth defects with *mcm10-1*. Deletion of *srs2* is synthetically lethal with *mcm10-1*, as *mcm10 srs2* is viable only when it carries a plasmid containing the wild-type *MCM10* gene. The strain is unable to grow on 5-FOA when the plasmid is lost due to the *URA3* marker. *mcm10 sgs1*, *mcm10 exo1*, and *mcm10 srs2* synthetic growth defects are suppressed by *mcm2-G400D*, whereas those caused by *mcm10 mre11* and *mcm10 rad50* are not suppressed.

Rad53 and Mec1 are both key players in the checkpoint signaling pathway that have a role in stabilizing stalled forks as well as in transducing signals to downstream effectors (for a review, see reference 4). Deletion of *rad53* and *mec1* greatly diminished the ability of the *mcm2* mutants to suppress *mcm10* TS. These results suggest that the checkpoint pathway is activated in *mcm10 mcm2*. Phosphorylation of Rad53 is required for replication fork stabilization.

To determine if Rad53 is indeed activated, we examined the phosphorylation state of Rad53 in *mcm10-1*, *mcm2-G400D*, and *mcm10 mcm2* mutants. Log-phase cells were grown at 37°C for 2 h and collected for protein extraction and Western

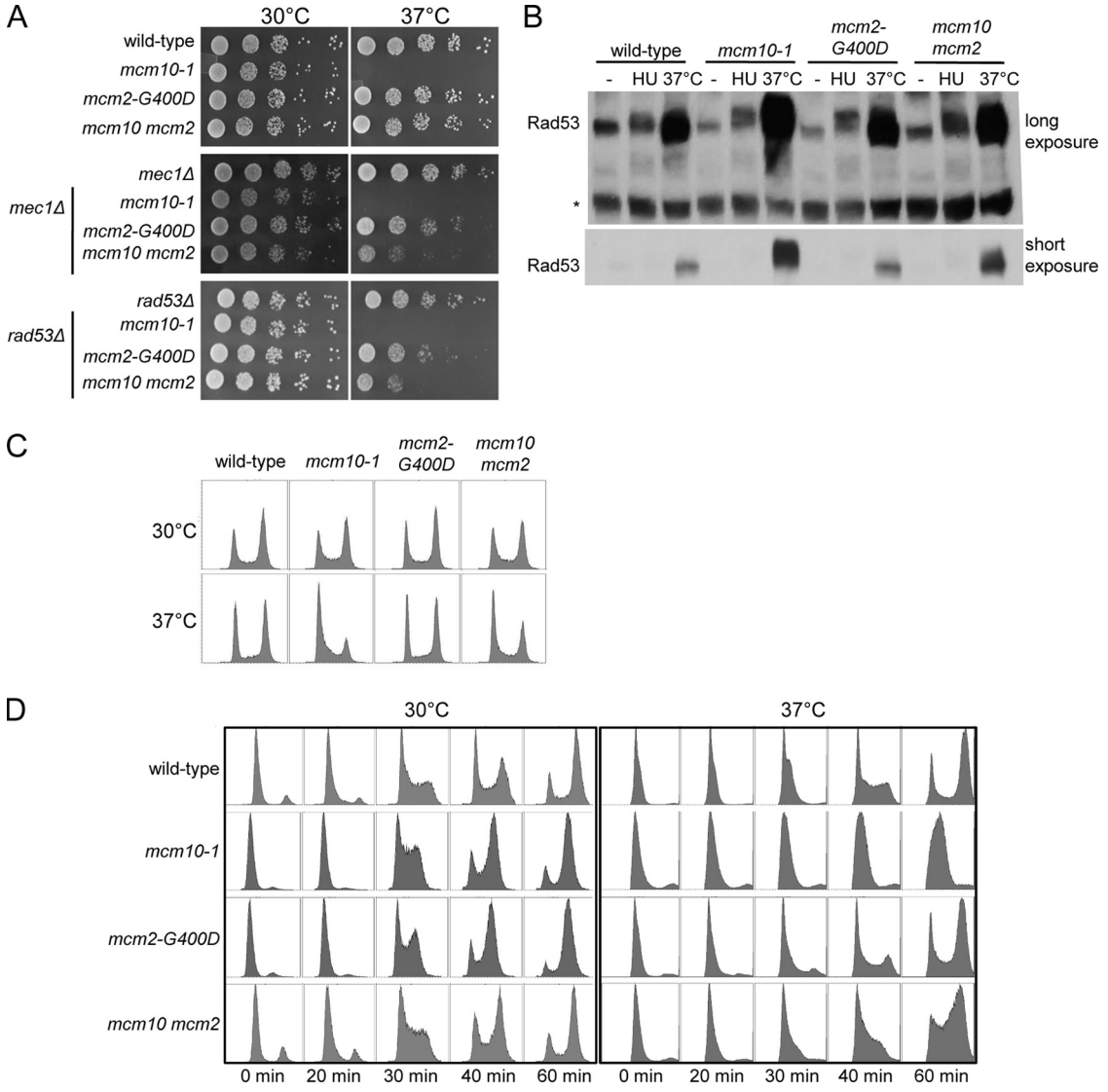

FIG. 5. Checkpoint functions are required for viability of *mcm10 mcm2*. (A) Serial dilutions of cells are spotted onto YPD and incubated at 30°C or 37°C. Deletion of *MEC1* and *RAD53* has a negative effect on suppression. (B) Rad53 phosphorylation in *mcm10-1* and *mcm10 mcm2*. 3×HA-tagged Rad53 strains with *mcm10-1* and *mcm2-G400D* mutations were grown to log phase, arrested by α-factor for 1.5 h, and released into fresh media with or without HU at 30°C for 1 h or without HU at 37°C for 1 h. Samples were collected for Western blot analysis to assay the phosphorylation state of Rad53. Exposure of *mcm10-1* to 37°C leads to hyperphosphorylation of Rad53. Suppression of TS by *mcm2* is accompanied by a decrease in Rad53 phosphorylation. (C) FACS analysis of wild-type, *mcm10-1*, *mcm2-G400D*, and *mcm10 mcm2* cells. For overall ratio of cells in G_1, S, or G_2 phase, log-phase cells of wild-type, *mcm10-1*, *mcm2-G400D*, and *mcm10 mcm2* strains were collected without α-factor arrest. (D) Analysis of cell cycle progresses was carried out by arresting the cells at G_1 and releasing into S phase at either 30°C or 37°C. Samples analyzed at 37°C were preincubated at 37°C during α-factor arrest to allow time for Mcm10 protein degradation. At 37°C, with Mcm10 depletion, significant delay in S-phase entry and progression was observed as published previously (29). While *mcm2* cells do not show any difference in cell cycle progression from that of wild-type cells, a slight delay of S-phase progression in *mcm10 mcm2* cells was observed.

blot analysis (Fig. 5B). We found that Rad53 is hyperphosphorylated in the *mcm10* mutant at 37°C. Previous work showed that a shift to 37°C causes an irreversible loss of viability upon return to permissive temperature in *mcm10* cells (2). Therefore, degradation of Mcm10p, which causes irreparable DNA damage, must have activated Rad53. In the *mcm10 mcm2* mutant, Rad53 is also phosphorylated, though the shift due to phosphorylation is much weaker. While Rad53 is activated in both *mcm10* and *mcm10 mcm2* mutants, the consequences of its activation are drastically different, as the *mcm10* mutant loses viability, while the *mcm10 mcm2* mutant is phenotypically similar to the wild type. Rad53 phosphorylation is not enhanced in the *mcm2* mutant, ruling out the possibility that the mutation in the helicase alone activates the checkpoint pathway. It appears that the *mcm2* mutant helicase in combination with *mcm10* causes activation of Rad53 that prevents or corrects the damage by *mcm10*. Our results suggest that the unstable replication fork in *mcm10* is stabilized by the *mcm2* suppressor and a mechanism that involves activation of the checkpoint pathway.

Since activated Rad53 can slow down S phase to provide more time for repair of damages, we determined whether Rad53 activation in *mcm10 mcm2* cells is accompanied by a slower S phase by FACS analysis. To obtain the overall ratio of cells in G_1, S, or G_2 phase, log-phase cells of wild-type, *mcm10-1*, *mcm2-G400D*, and *mcm10 mcm2* strains were collected without α-factor arrest. At 30°C, the overall ratios of G_1/S/G_2-phase cells are similar for all strains, with two peaks at G_1 and G_2 phases with the G_2-phase peak being slightly stronger (Fig. 5C). However, at 37°C, in the *mcm10* cells, the G_1 peak is much greater than the G_2 peak, suggesting that the cells have difficulty entering S phase. This problem seems to be corrected in *mcm2-G400D* cells, though not completely, as the G_1 peak is still stronger than the G_2 peak. A closer examination of how the cell cycle progresses was carried out by arresting the cells at G_1 phase and releasing into S phase at either 30°C or 37°C (Fig. 5D). At 37°C, with Mcm10 depletion, significant delay in S-phase entry and progression was observed as reported previously (29). While *mcm2* cells do not show any significant difference in cell cycle progression from the wild type, a slight delay of S-phase progression in *mcm10 mcm2* cells was observed. Entry into S phase seemed to be similar for all strains, as they entered S phase at the 30-min time point. However, the delay in progression was evident, because *mcm10 mcm2* cells were still in S phase while wild-type or *mcm2* cells were already into G_2 phase at the 60-min time point. Therefore, the S-phase delay in *mcm10 mcm2* cells is consistent with the checkpoint activation and ongoing DNA repair.

Mutations in *MCM2* stabilize Cdc17p in *mcm10* cells in a checkpoint-dependent manner. Cdc17 is the catalytic subunit of the Polα primase, the only DNA polymerase that has the capability of *de novo* DNA synthesis (6). The primase is required for priming Okazaki fragments on the lagging strand throughout elongation. In budding yeast, it is suggested that Mcm10 functions as a linker between the Polα primase and the helicase, because Mcm10 is required for Cdc17 stabilization and its association with chromatin (33). In both *mcm10-1* and *mcm10* temperature-degron (TD) mutants, Mcm10 protein degradation at 37°C was accompanied by Cdc17 degradation with similar kinetics (33). We found that the *mcm2* suppressors did not suppress degradation of the mutant Mcm10 protein (Fig. 3B). However, since the primase activity is indispensable for DNA replication, we reasoned that suppression of *mcm10* TS by *mcm2* must be accompanied by restoration of Cdc17 function, either directly or indirectly. Therefore, we performed Western blot experiments with Cdc17-3xHA-tagged wild-type, *mcm10-1*, and *mcm10-1 mcm2-G400D* strains to determine the stability of Cdc17p. We found that while the *mcm2* suppressor failed to stabilize Mcm10 in *mcm10-1* cells, it was able to stabilize Cdc17 (Fig. 6A).

Since Mcm10 is suggested to be a chaperone for Cdc17 stability, it was of interest how Cdc17 is stabilized despite Mcm10 instability. Two-hybrid analysis did not show interaction between Mcm2-G400D and Cdc17, suggesting that the Mcm2 suppressor is not directly involved in the stabilization of Cdc17 by establishing new interactions. We had noticed that suppression of *mcm10-1* TS by *mcm2-G400D* was greatly diminished in a *mec1* or *rad53* null background, suggesting that the checkpoint function may be required for Cdc17 stability. We tested this idea by examining Cdc17 stability in *mec1* and in *rad53* cells. We carried out Western blot analysis of Cdc17-3xHA to determine protein stability in *mec1*Δ *mcm10 mcm2* and *rad53*Δ *mcm10 mcm2* cells, respectively (Fig. 6B). We found that Cdc17 was no longer stable when Mec1 function was lost. However, loss of Rad53 did not affect Cdc17 stability. This result suggests that stability of Cdc17 in *mcm10 mcm2* cells depends on a specific function of Mec1 in stabilizing the replication fork.

As degradation of Cdc17 would lead to cessation of DNA synthesis on the lagging strand, ssDNA is expected to accumulate at the fork in *mcm10-1* at 37°C. To examine ssDNA at replication forks, we visualized RPA-YFP localization in log-phase cells of wild-type, *mcm10-1*, *mcm2-G400D*, and *mcm10 mcm2* strains at either 30°C or 37°C (Fig. 6C, panel i). The frequencies of RPA foci observed in S-phase cells in these different strains are compared in a bar graph (Fig. 6C, panel ii). In *mcm10-1* cells, we observed intense RPA focus formation, and the number of cells with RPA foci increased with temperature. Importantly, *mcm2-G400D*, which does not display RPA focus formation on its own, suppresses RPA focus formation in *mcm10-1* cells, as the level of focus formation in *mcm10 mcm2* cells at 37°C is similar to that of *mcm10-1* cells at 30°C. This decrease in RPA focus formation suggests that the mutant helicase is preventing ssDNA accumulation that results from the loss of Mcm10.

DISCUSSION

The properties of Mcm10, its role in Cdc17 stability and association at the fork (33), and its interaction with the MCM helicase all suggest that Mcm10 plays a pivotal role in physically linking and coordinating the activities of polymerase α primase and the MCM helicase. We reasoned that suppression of the loss of this linker function would involve either restoration of Mcm10 function or recruiting another pathway to coordinate the polymerase and helicase activities. The finding that *mcm2* suppressors do not restore the interaction of Mcm2 with the mutant Mcm10 protein or stabilize the mutant Mcm10 protein suggests that the latter is more likely. In achieving this end, the mutant helicase has to play a critical role. Although no detectable physiological defect is observed in the *mcm2-G400D* suppressor other than the mild *mcm* defect, the archaeal MCM helicase bearing the suppressor mutations invariably showed a compromised helicase activity. This result suggests that the altered helicase activity is critical for the suppression of the conditional lethality of *mcm10*.

What are the phenotypes associated with the *mcm10* conditional lethality? They should be phenotypes that are also suppressed by the *mcm2* suppressors. We showed that *mcm2* suppresses the replication fork pausing phenotype as well as HU and MMS sensitivity of *mcm10*. Furthermore, it suppresses the synthetic growth defects of the loss of Sgs1, Exo1, or Srs2, a cohort of DNA helicases/nucleases, in *mcm10* strains. These helicases/nucleases are involved in DSB repair (DSBR) in two capacities: (i) through resolution of aberrant fork structures to prevent DSB formation, and (ii) through resection of DSBs after their formation (19, 30, 41). In contrast, *mcm2-G400D* fails to suppress the synthetic growth defects of *mcm10 mre11* or *mcm10 rad50* strains. Mre11 and Rad50 are the major

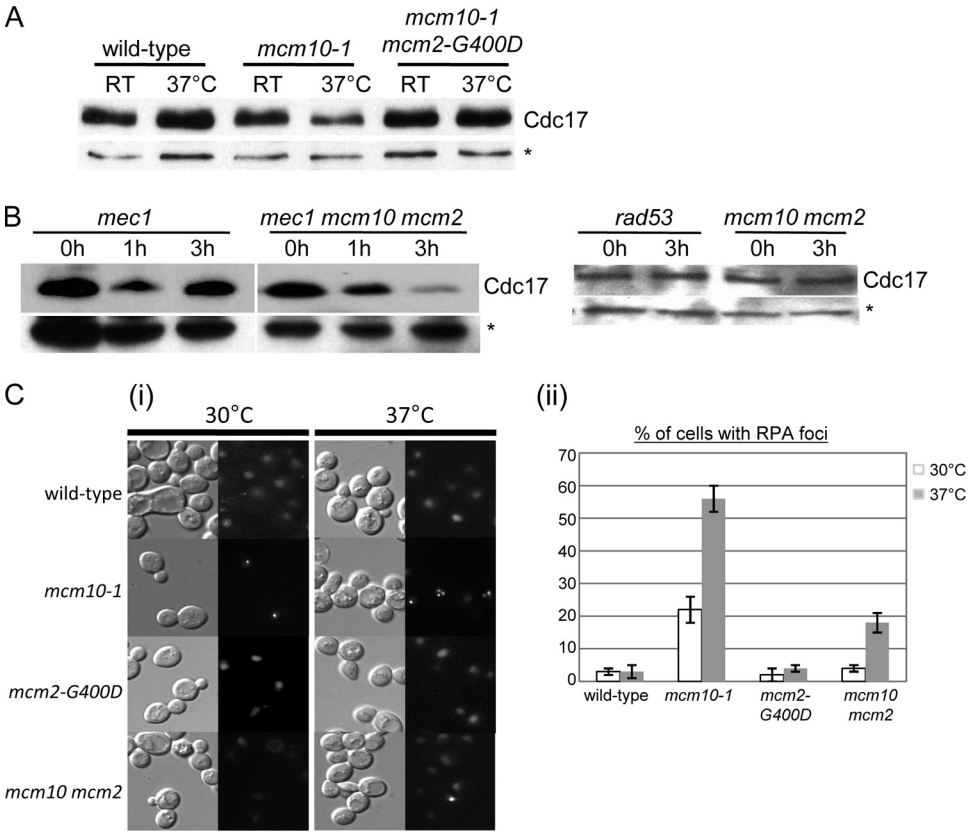

FIG. 6. *mcm2-G400D* stabilizes Cdc17 in a Mec1-dependent manner. (A) Log-phase cells were incubated at either room temperature or 37°C for 90 min and collected for Western blot analysis. Cdc17 is unstable in *mcm10-1* cells at 37°C but stabilized in *mcm2-G400D mcm10-1* cells. (B) Log-phase cells of *mec1* and *mec1 mcm10-43 mcm2-G400D* strains were incubated at 37°C for 0, 1, and 3 h and harvested for Western blot analysis. Loss of Mec1 function in *mcm10-43 mcm2-G400D* cells leads to degradation of Cdc17. Log-phase cells of *rad53* and *rad53 mcm10-43 mcm2-G400D* strains were incubated at 37°C for 0 and 3 h and before being harvested for Western blot analysis. Loss of Rad53 function has no effect on Cdc17 stability. Asterisk indicates the cross-reacting band, which serves as a loading control. (C) (i) Log-phase cells of *RFA1-YFP* wild-type, *mcm10-1*, *mcm2-G400D*, and *mcm10 mcm2* strains were grown at either 30°C or 37°C and subjected to microscopy analysis. The extent of RPA focus formation in *mcm10-1* cells increased with the temperature, and *mcm2-G400D* suppressed this. (ii) The percentage of cells with RPA foci was quantified by averaging three independent counts of >100 cells. The level of RPA focus formation in *mcm10 mcm2* cells at 37°C was similar to that in *mcm10-1* cells at 30°C.

proteins involved in all DSB repair. The differences in requirement of these DSBR proteins in the suppression of *mcm10* by *mcm2* suggest that *mcm2* is able to either substitute for Sgs1, Exo1, and Srs2 in the repair of their DSB substrates or prevent the formation of these substrates. The roles of Sgs1 and Exo1 are well defined in the DSB repair pathway, so it is doubtful that a defective MCM helicase could carry out their functions, especially those involving nuclease activities. A more likely scenario is that *mcm2* is preventing the formation of aberrant fork structures and thereby abrogates the need for these helicases/nucleases. Under this scenario, we imagine that reduced activity of the helicase prevents the formation of a subset of DNA damage due to aberrant fork structures caused by the instability of Mcm10-1.

Mec1 is important for preventing dissociation of fork components, polymerase α in particular, when replication forks stall under replication stress (9). It was shown that Mec1, rather than Rad53, plays a key role in maintaining the association of Polα with the replication fork when forks stall. Therefore, the Mec1-dependent stabilization of Cdc17 in *mcm10 mcm2* cells suggests that preventing fork collapse is a key factor in preserving the viability of cells despite loss of Mcm10 function. Though it is possible that the Mcm2 suppressor stabilizes Cdc17 by acquiring the ability to interact directly between Polα and the helicase, two-hybrid analysis of Cdc17 with either wild-type or mutant Mcm2 does not support this hypothesis (data not shown). We believe that normally Mcm10 may stabilize Polα by direct interaction, but in the event that Mcm10 fails to carry out this function, alternative pathways may be evoked to substitute for this critical activity. An alternative explanation is that the stability of Polα depends on fork integrity as a whole rather than interaction with any particular protein and that cells are multifaceted in maintaining the integrity of the replication fork under normal or stress conditions.

In summary, our study suggests that reduced MCM helicase activity rendered by the *mcm2* suppressor mutation is able to mediate fork stabilization by activating the checkpoint pathway and coordinating the helicase and polymerase activities in the absence of Mcm10. A model of how *mcm2* may suppress *mcm10* is shown in Fig. 7. In a normal replication fork, Mcm10, by interaction with both Polα and the MCM helicase, coordi-

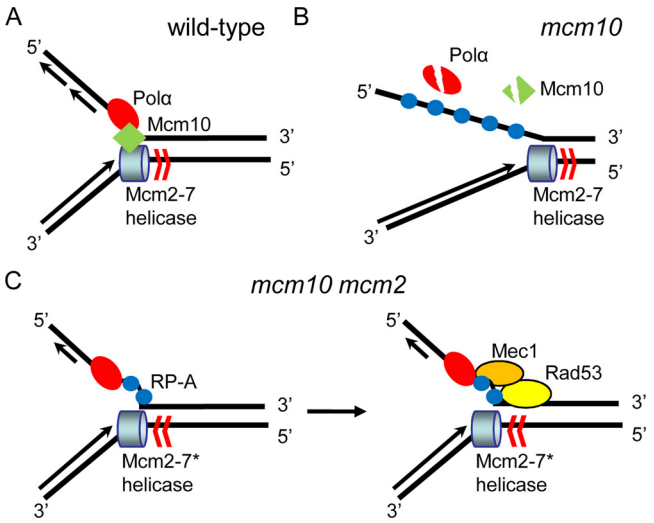

FIG. 7. Model of mechanism by which *mcm2* suppresses *mcm10* conditional lethality. (A) Mcm10 couples helicase to Polα primase under normal replication conditions. (B) Degradation of Mcm10 causes dissociation of Polα from chromatin and failure to coordinate the unwinding activity with the polymerizing activity result in the exposure of ssDNA, fork collapse, and checkpoint activation. (C) Mutation in the helicase compromises the unwinding activity, allowing the polymerase to keep up without a coupling factor. The imperfect synchrony results in chronic exposure of ssDNA that renders the fork "prone to checkpoint activation" but able to remain intact. The checkpoint proteins recruited to the fork help stabilize the components of the fork and replace the function of Mcm10 as a coupler.

nates the polymerizing and unwinding activities on the lagging strand (Fig. 7A). In the *mcm10* mutant, Mcm10 is unstable at 37°C, resulting in the decoupling of Polα from the helicase. Polα released from chromatin is destabilized. The uncoordinated unwinding and polymerizing activities expose extensive ssDNA (Fig. 6C), especially on the lagging strand, resulting in fork collapse and other damage that cannot be rescued by checkpoint-activated repair (Fig. 7B). We imagine that *mcm2* suppresses the *mcm10* conditional lethality by preventing such irreversible damage. The suppressor mutations may alter the rate of helicase unwinding to the extent that ssDNA accumulation is reduced and fork collapse is diverted; however, coordination between the unwinding and polymerizing activities may still be imperfect. As a result, chronic activation of checkpoint response in *mcm10 mcm2* (Fig. 5B) by persistent low-level ssDNA exposure works in the favor of the faulty replication fork by stabilizing it (Fig. 7C). In other words, we propose that the loss of physical stabilization at the fork caused by the unstable Mcm10 can be compensated for by a mechanistic stabilization that results from the compromised helicase and the activated checkpoint proteins to coordinate the lagging strand synthesis. This hypothesis points to the dynamics of fork components in adapting to the defects of one another and the integration of different cellular pathways, such as replication, repair, and checkpoints, to maintain the integrity of the genome.

ACKNOWLEDGMENTS

We thank a very talented group of undergraduate and rotation students, Alice Leung, Mike Singer, Jany Chan, and Stephanie Yazinski, for identifying many of the suppressor alleles. We thank Nozomi Sakakibara for her help in the construction of the Mth mutants. We also thank Marcus Smolka and Francisco M. Bastos de Oliviera for their intellectual and technical input, especially with regard to checkpoint effects. Lastly, we thank the Huberman lab for their patience and time in teaching C.L. the 2D gel technique.

This work was supported by NSF (MBG-0453773) and NIH GM072557 awarded to B.K.T. and NSF (MCB-0815646) awarded to Z.K.

REFERENCES

1. **Alcasabas, A. A., A. J. Osborn, J. Bachant, F. Hu, P. J. H. Werler, K. Bousset, K. Furuya, J. F. X. Diffley, A. M. Carr, and S. J. Elledge.** 2001. Mrc1 transduces signals of DNA replication stress to activate Rad53. Nat. Cell Biol. **3:**958–965.
2. **Araki, Y., Y. Kawasaki, H. Sasanuma, B. K. Tye, and A. Sugino.** 2003. Budding yeast *mcm10/dna43* mutant requires a novel repair pathway for viability. Genes Cells **8:**465–480.
3. **Bailey, S., W. K. Eliason, and T. A. Steitz.** 2007. Structure of hexameric DnaB helicase and its complex with a domain of DnaG primase. Science **318:**459–463.
4. **Branzei, D., and M. Foiani.** 2008. Regulation of DNA repair throughout the cell cycle. Nat. Rev. Mol. Cell Biol. **9:**297–308.
5. **Brewster, A. S., G. Wang, X. Yu, W. B. Greenleaf, J. M. Carazo, M. Tjajadi, M. G. Klein, and X. S. Chen.** 2008. Crystal structure of a near-full-length archaeal MCM: functional insights for an AAA+ hexameric helicase. Proc. Natl. Acad. Sci. USA **105:**20191–20196.
6. **Burgers, P. M. J.** 1998. Eukaryotic DNA polymerases in DNA replication and DNA repair. Chromosoma **107:**218–227.
7. **Byun, T. S., M. Pacek, M.-C. Yee, J. C. Walter, and K. A. Cimprich.** 2005. Functional uncoupling of MCM helicase and DNA polymerase activities activates the ATR-dependent checkpoint. Genes Dev. **19:**1040–1052.
8. **Chattopadhyay, S., and A.-K. Bielinsky.** 2007. Human Mcm10 regulates the catalytic subunit of DNA polymerase α and prevents DNA damage during replication. Mol. Biol. Cell **18:**4085–4095.
9. **Cobb, J. A., L. Bjergbaek, K. Shimada, C. Frei, and S. M. Gasser.** 2003. DNA polymerase stabilization at stalled replication forks requires Mec1 and the RecQ helicase Sgs1. EMBO J. **22:**4325–4336.
10. **Desany, B. A., A. A. Alcasabas, J. B. Bachant, and S. J. Elledge.** 1998. Recovery from DNA replicational stress is the essential function of the S-phase checkpoint pathway. Genes Dev. **12:**2956–2970.
11. **Dijkwel, P. A., J. P. Vaughn, and J. L. Hamlin.** 1991. Mapping of replication initiation sites in mammalian genomes by two-dimensional gel analysis: stabilization and enrichment of replication intermediates by isolation on the nuclear matrix. Mol. Cell. Biol. **11:**3850–3859.
12. **Donato, J. J., S. C. C. Chung, and B. K. Tye.** 2006. Genome-wide hierarchy of replication origin usage in *Saccharomyces cerevisiae*. PLoS Genet. **2:**e141.
13. **Fields, S., and O. Song.** 1989. A novel genetic system to detect protein-protein interactions. Nature **340:**245–256.
14. **Fien, K., Y.-S. Cho, J.-K. Lee, S. Raychaudhuri, I. Tappin, and J. Hurwitz.** 2004. Primer utilization by DNA polymerase {alpha}-primase is influenced by its interaction with Mcm10p. J. Biol. Chem. **279:**16144–16153.
15. **Gangloff, S., C. Soustelle, and F. Fabre.** 2000. Homologous recombination is responsible for cell death in the absence of the Sgs1 and Srs2 helicases. Nat. Genet. **25:**192–194.
16. **Hamdan, S. M., D. E. Johnson, N. A. Tanner, J.-B. Lee, U. Qimron, S. Tabor, A. M. van Oijen, and C. C. Richardson.** 2007. Dynamic DNA helicase-DNA polymerase interactions assure processive replication fork movement. Mol. Cell **27:**539–549.
17. **Homesley, L., M. Lei, Y. Kawasaki, S. Sawyer, T. Christensen, and B. K. Tye.** 2000. Mcm10 and the MCM2-7 complex interact to initiate DNA synthesis and to release replication factors from origins. Genes Dev. **14:**913–926.
18. **Huberman, J. A.** 1997. Mapping replication origins, pause sites, and termini by neutral/alkaline two-dimensional gel electrophoresis. Methods **13:**247–257.
19. **Ira, G., A. Malkova, G. Liberi, M. Foiani, and J. E. Haber.** 2003. Srs2 and Sgs1Top3 suppress crossovers during double-strand break repair in yeast. Cell **115:**401–411.
20. **Ira, G., A. Pellicioli, A. Balijja, X. Wang, S. Fiorani, W. Carotenuto, G. Liberi, D. Bressan, L. Wan, N. M. Hollingsworth, J. E. Haber, and M. Foiani.** 2004. DNA end resection, homologous recombination and DNA damage checkpoint activation require CDK1. Nature **431:**1011–1017.
21. **Kasiviswanathan, R., J.-H. Shin, E. Melamud, and Z. Kelman.** 2004. Biochemical characterization of the *Methanothermobacter thermautotrophicus* minichromosome maintenance (MCM) helicase N-terminal domains. J. Biol. Chem. **279:**28358–28366.
22. **Katou, Y., Y. Kanoh, M. Bando, H. Noguchi, H. Tanaka, T. Ashikari, K. Sugimoto, and K. Shirahige.** 2003. S-phase checkpoint proteins Tof1 and Mrc1 form a stable replication-pausing complex. Nature **424:**1078–1083.
23. **Kawasaki, Y., S.-I. Hiraga, and A. Sugino.** 2000. Interactions between Mcm10p and other replication factors are required for proper initiation and

elongation of chromosomal DNA replication in Saccharomyces cerevisiae. Genes Cells **5:**975–989.
24. **Krejci, L., S. Van Komen, Y. Li, J. Villemain, M. S. Reddy, H. Klein, T. Ellenberger, and P. Sung.** 2003. DNA helicase Srs2 disrupts the Rad51 presynaptic filament. Nature **423:**305–309.
25. **Kushnirov, V. V.** 2000. Rapid and reliable protein extraction from yeast. Yeast **16:**857–860.
26. **Lee, J.-K., Y.-S. Seo, and J. Hurwitz.** 2003. The Cdc23 (Mcm10) protein is required for the phosphorylation of minichromosome maintenance complex by the Dfp1-Hsk1 kinase. Proc. Natl. Acad. Sci. USA **100:**2334–2339.
27. **Liachko, I., and B. K. Tye.** 2005. Mcm10 is required for the maintenance of transcriptional silencing in Saccharomyces cerevisiae. Genetics **171:**503–515.
28. **Lou, H., M. Komata, Y. Katou, Z. Guan, C. C. Reis, M. Budd, K. Shirahige, and J. L. Campbell.** 2008. Mrc1 and DNA polymerase [var epsilon] function together in linking DNA replication and the S phase checkpoint. Mol. Cell **32:**106–117.
29. **Merchant, A., Y. Kawasaki, Y. Chen, M. Lei, and B. Tye.** 1997. A lesion in the DNA replication initiation factor Mcm10 induces pausing of elongation forks through chromosomal replication origins in *Saccharomyces cerevisiae*. Mol. Cell. Biol. **17:**3261–3271.
30. **Mimitou, E. P., and L. S. Symington.** 2008. Sae2, Exo1 and Sgs1 collaborate in DNA double-strand break processing. Nature **455:**770–774.
31. **Nyberg, K. A., R. J. Michelson, C. W. Putnam, and T. A. Weinert.** 2002. Toward maintaining the genome: DNA damage and replication checkpoints. Annu. Rev. Genet. **36:**617–656.
32. **Paull, T. T., and M. Gellert.** 1998. The 3′ to 5′ exonuclease activity of Mre11 facilitates repair of DNA double-strand breaks. Mol. Cell **1:**969–979.
33. **Ricke, R. M., and A.-K. Bielinsky.** 2004. Mcm10 regulates the stability and chromatin association of DNA polymerase-α. Mol. Cell **16:**173–185.
34. **Sawyer, S. L., I. H. Cheng, W. Chai, and B. K. Tye.** 2004. Mcm10 and Cdc45 cooperate in origin activation in Saccharomyces cerevisiae. J. Mol. Biol. **340:**195–202.
35. **Shechter, D., V. Costanzo, and J. Gautier.** 2004. Regulation of DNA replication by ATR: signaling in response to DNA intermediates. DNA Repair **3:**901–908.
36. **Shin, J.-H., B. Grabowski, R. Kasiviswanathan, S. D. Bell, and Z. Kelman.** 2003. Regulation of minichromosome maintenance (MCM) helicase activity by Cdc6. J. Biol. Chem. **278:**38059–38067.
37. **Sogo, J. M., M. Lopes, and M. Foiani.** 2002. Fork reversal and ssDNA accumulation at stalled replication forks owing to checkpoint defects. Science **297:**599–602.
38. **Tercero, J. A., and J. F. X. Diffley.** 2001. Regulation of DNA replication fork progression through damaged DNA by the Mec1/Rad53 checkpoint. Nature **412:**553–557.
39. **Tercero, J. A., M. P. Longhese, and J. F. X. Diffley.** 2003. A central role for DNA replication forks in checkpoint activation and response. Mol. Cell **11:**1323–1336.
40. **Wu, J., and D. Gilbert.** 1995. Rapid DNA preparation for 2D gel analysis of replication intermediates. Nucleic Acids Res. **23:**3997–3998.
41. **Zhu, Z., W.-H. Chung, E. Y. Shim, S. E. Lee, and G. Ira.** 2008. Sgs1 helicase and two nucleases Dna2 and Exo1 resect DNA double-strand break ends. Cell **134:**981–994.
42. **Zou, L., and S. J. Elledge.** 2003. Sensing DNA damage through ATRIP recognition of RPA-ssDNA complexes. Science **300:**1542–1548.